Title: Supramolecular block copolymers as novel UV and NIR responsive nanocarriers based on a photolabile coumarin unit

Authors:

Alejandro Roche,[a] Emmanuel Terriac,[b] Rosa M. Tejedor,[a,c] Luis Oriol,[a] Aránzazu del Campo,[b,d] Milagros Piñol[a*]

Affiliations:

[a]Departamento de Química Orgánica, Instituto de Ciencia de Materiales de Aragón (ICMA), Universidad de Zaragoza-CSIC, c/ Pedro Cerbuna 12, 50009, Zaragoza, Spain

[b]INM – Leibniz Institute for New Materials, Campus D2 2, 66123 Saarbrücken, Germany

[c]Centro Universitario de la Defensa, Academia General Militar, Ctra. de Huesca s/n, 50090, Zaragoza, Spain

[d]Chemistry Department, Saarland University, 66123 Saarbrücken, Germany

Corresponding author: Milagros Piñol, mpinol@unizar.es

Highlights

A versatile supramolecular approach to coumarin-containing block copolymers is described

Encapsulation and UV and NIR photorelease properties of polymeric micelles has been studied

Light response of supramolecular nanocarriers is similar to covalent materials.

Abstract

A new series of amphiphilic block copolymers has been prepared by ring opening polymerization (ROP) of cyclic carbonates using PEG as initiator. The light responsive unit [7-(diethylaminocoumarin)-4-yl]methyl ester has been introduced by a modular and versatile supramolecular approach, while a reference covalent copolymer has been synthesized for the shake of comparison. Synthesized copolymers showed monomodal narrow distributions and were able to self-assemble into spherical micelles when dispersed in water. UV irradiation allowed us the modification of the self-assemblies morphology, as proved by means of fluorescence spectroscopy, dynamic light scattering (DLS) and transmission electron microscopy (TEM). Both the supramolecular and covalent functionalized block copolymers were able to encapsulate small fluorescent probes as payload and to release them upon UV and NIR irradiation.

Keywords: light responsive; block copolymers; coumarin; nanocarriers; self-assembly

1. Introduction

Polymeric nanoparticles have been considered attractive nanocarriers for regulated release of drugs as a way to overcome toxicity and solubility issues associated with high drug dosages, and improval of target selectivity by modifying the surface of the carrier for directed delivery [1-6]. Amongst several possibilities, polymer micelles usually formed by spontaneous assembly of amphiphilic block copolymers (BCs) in water have appeared particularly attractive to encapsulate and transport small hydrophobic drugs for biomedical purposes. One of the reasons is that, due to their small size (usually < 100 nm), polymer micelles might accumulate at tumors sites through passive targeting by the enhanced permeation and retention (EPR) effect [7,8]. Besides, their size, stability or drug laoding ability can be tuned by changing structural parameters such as the chemical nature and length of the polymeric segments [3,9] that in turn can be precisely adjusted combining controlled polymerizations techniques with postpolymerization modification strategies [10,11].

Performance of the polymeric micelles can be enhanced by incorporating sensitive units in the nanoparticle (to pH, temperature, light or to a chemical) so externally regulated delivery of the drug can be realized. Light is a rapid, noninvasive, and clean stimulus that can be spatially and temporally controlled. By introducing a photosensitive unit as a pendant substituent of the hydrophobic block, light action has been used to induced the destabilization of the micellar assemblies and the concurrent release of any encapsulated active [12-16]. A variety of light responsive units have been tested for this purpose including azobenzenes, spiropyrans, o-nitrobenzyl esters or coumarin esters [17-22]. In most of these cases, release is activated with UV light but to avoid the phototoxicity effects of UV exposure and increase penetration depth in tissues, near

infrared (NIR) stimulation is preferred for biomedical applications [23,34]. Thus, the organic units 2-diazonaphtoquinone (DNQ) [25,26] and o-nitrobenzyl esters [27] have been integrated in micellar systems to release hydrophobic cargoes under NIR (*via* two-photon absorption) light stimulation. Because of its large two-photon absorption cross section, amphiphilic BCs with the [7-(diethyaminocoumarin)-4-yl]methyl ester moiety have also been investigated [28,29]. Micelles formed by amphiphilic BC of poly(ethylene glycol) and a coumarin polymethacrylate were able to release a fluorescent probe under NIR light induced cleavage of the coumarin ester [28]. Also BCs containing a coumarin functionalized polypeptide have shown to enable NIR light release of Rifampicin and Paclitaxel [29].

To engineer stimuli-responsive polymers, different postpolymerization modification chemistries have been proposed [30-32]. In this context, noncovalent postpolymerization modifications to incorporate lateral functionalities are interesting approaches as they allow great versatility at minimum synthetic cost [33-35]. Hydrogen bond mediated side chain functionalization is of particular relevance due to its strength and directionality, specially when multiple hydrogen bonds are formed together. Highly specific interactions between nucleobases or analogues pairs with complementary hydrogen bond have been exploited to adjust the properties of supramolecular polymers and their self-assembly abilities [36]. Inspired by the work of Rotello and co-workers with the 2,6-diacylaminopyridine/thymine pair (DAP/T) [37], we recently described the light induced release ability of assemblies of supramolecular amphiphilic block copolymers [17]. The polymers were formed by a poly(ethylene glycol) hydrophilic segment and a polymethacrylate hydrophobic segment with pendant 2,6-diacylaminopyridine units to which a thymine 4-isobutyloxyazobenzene was grafted

through a triple H-bond. The self-assemblies were used to load and trigger the delivery of small fluorescent molecules under UV light stimulation.

In an extension of this approach, here we report on a series of light-responsive BCs consisting of a degreadable aliphatic polycarbonate hydrophobic blocks that can be functionalized with UV/NIR-cleavable coumarins either by covalent or noncovalent approaches. Aliphatic polycarbonates show low toxicity, biotoxicity, biocompatibility and biodegradability. Besides, they are readily affordable by ring opening polymerization (ROP) of cyclic carbonate monomers with pendant alkyne and alkene functional groups, which allows to introduce additional functionalities [38-42], i.e. by thiol-ene [43-45] or Cu(I) catalyzed azide-alkyne cycloaddition (CuAAC) chemistries [46,47].

Directed by the above mentioned issues, the objective of the present work was the fabrication of NIR light triggered drug delivery systems from supramolecular degradable amphiphilic BCs focussing on the [7-(diethyaminocoumarin)-4-yl]methyl ester NIR sensitive group, previously validated by Zhao and co-workers [28,29]. To circumvent tedious synthesis of coumarin monomers and to avoid the use of metallic catalysts, we devised a modular synthetic approach where the lateral anchoring of the light responsive coumarin by H-bond recognition using the DAP/T motif (Figure 1). For this purpose, we combined the organocatalyzed ROP of a cyclic allyl carbonate with two sequential postpolymerization modification steps: (i) the covalent integration of the DAP nucleobase analogue by thiol-ene reaction, (ii) the noncovalent integration by H-bond of the light responsive coumarin with a thymine unit. Besides, a covalent model was prepared for comparative purposes using an alternative synthetic pathway (Figure 1) based on our experience on lateral functionalization using CuAAC chemistry [48,49].

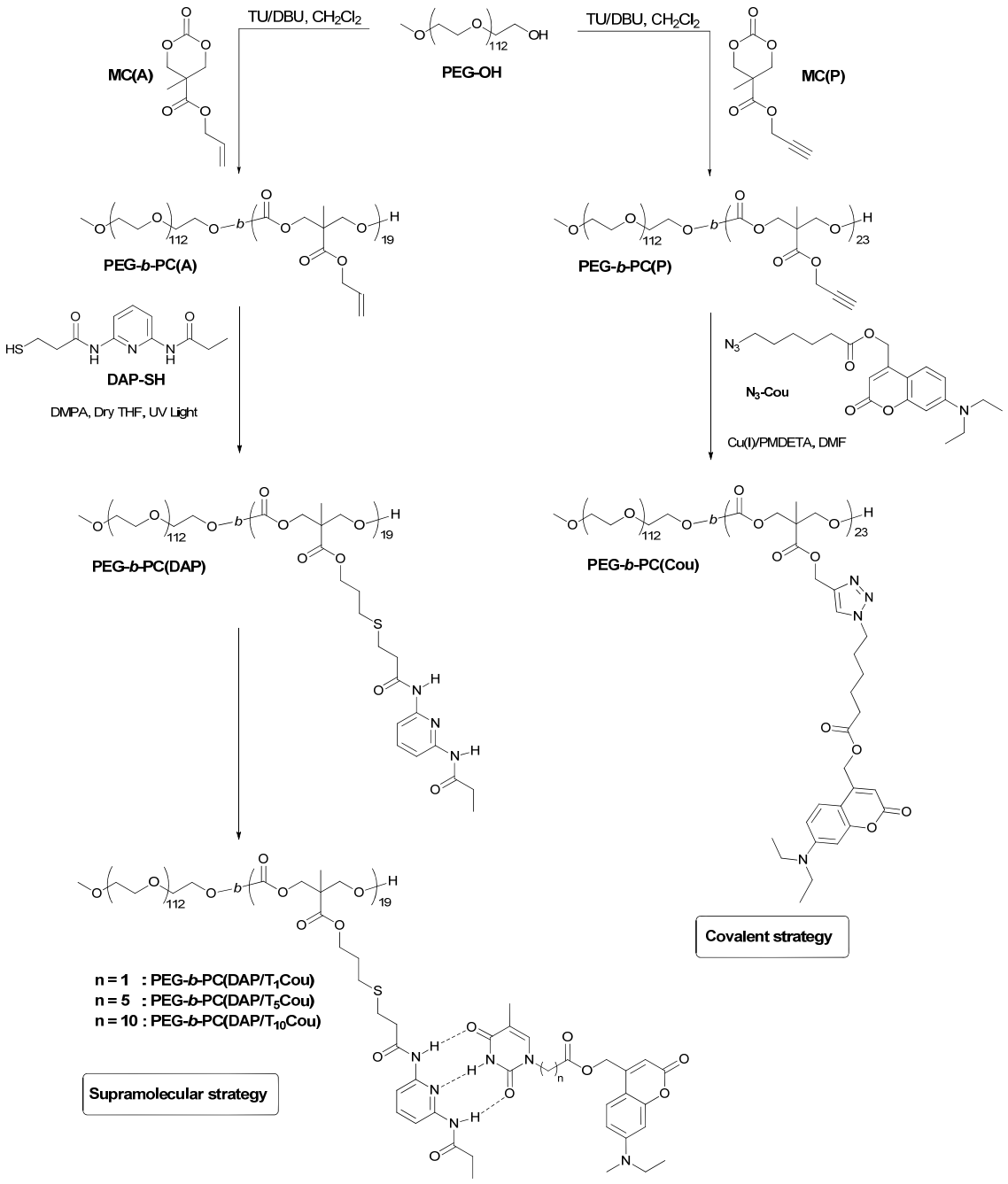

Figure 1. Synthesis pathway of coumarin functionalized block copolymers.

2. Experimental

2.1. Materials

Cyclic carbonates 5-methyl-5-allyloxycarbonyl-1,3-dioxan-2-one, MC(A), and 5-methyl-5-propargyloxycarbonyl-1,3-dioxan-2-one, MC(P) were synthesized according a previously reported procedure [50-52]. Synthesis and characterization of the

2,6-diacylaminopyridine thiol DAP-SH, coumarin thymines T_nCou and coumarin azide Cou-N_3 are described at the Supporting Information. Block copolymers PEG-*b*-PC(A) and PEG-*b*-PC(P) precursors were obtained by ROP using poly(ethylene glycol) methyl ether as the macroiniator as described in the literature [53]. Full details are given at the supporting information. Azobisisobutyronitrile (AIBN) was purchased from Fisher and rechrystallyzed in methanol prior to use. 2,2-Dimethoxy-2-phenylacetophenone (DMPA) and *N,N,N′,N″,N″*-pentamethyldiethylenetriamine (PMDETA) were purchased from Sigma Aldrich and used as received.

2.2. Synthesis of the coumarin functionalized supramolecular PEG-b-PC(DAP/TCou) and covalent PEG-b-PC(Cou) block copolymers

Synthesis of PEG-b-PC(DAP). A Schlenk flask was charged with DAP-SH (500 mg, 1.97 mmol), PEG-*b*-PC(A) (457 mg, 0.986 mmol of C=C) and DMPA (12.6 mg, 0.049 mmol) and flushed with Argon. Then, dry THF (5 mL) was added, and the solution stirred at 40 ºC for 4 h under 365 nm illumination. The reaction crude was purified by preparative SEC using Biobeds SX-1 and THF as eluent and, the polymer precipitated into cold diethyl ether and isolated by filtration as a white powder (90% yield). FTIR (KBr, υ cm^{-1}): 3316 (N-Hst), 2878 (C Csp^3–H), 1752 (C=O), 1701 (C=O), 1589, 1447, 1294, 1236. ^{1}H NMR (400 MHz, $CDCl_3$, δ, ppm): 8.90 - 8.12 (m, broad signal), 7.98 - 7.75 (m), 7.72 - 7.57 (m), 4.40 - 4.11 (m), 3.82 - 3.43 (m), 3.37 (s), 2.95 - 2.80 (m), 2.76 - 2.63 (m), 2.63 - 2.50 (m), 2.49 - 2.36 (m), 2.00 - 1.73 (m), 1.27 - 1.14 (m)

Synthesis of PEG-b-PC(DAP/TCou). A solution of TCou (25.4 mg, 0.061 mmol) and PEG-*b*-PC(DAP) (30.0 mg, 0.065 mmol) in dry THF (2 mL) was slowly evaporated at room temperature in an orbital shaker. The supramolecular polymer was dried under vacuum at 40 ºC overnight.

Synthesis of the coumarin functionalized covalent block copolymer PEG-b-PC(Cou). A Schlenk flask was charged with N_3-Cou (487 mg, 1.26 mmol), PEG-*b*-PC(P) (262 mg, 0.63 mmol of C≡C), CuBr (18.6 mg, 0.13 mmol) and PMDETA (22.52 mg, 0.13 mmol) and flushed with Argon. Then, deoxygenated and distilled *N,N*-dimethylformamide (5 mL) was added, and the solution stirred at 40 ºC for 72 h. The reaction crude was diluted with dichloromethane and washed three times with distilled water. The organic fraction was dried over $MgSO_4$, filtered and evaporated to dryness. Residual azide was removed by preparative SEC using Biobeds SX-1 and THF as eluent and, the polymer precipitated into cold diethyl ether and isolated by filtration as a pale yellow powder (80% yield). Extension of the modification was assessed by ^{1}H NMR from the disappearance of the alkynyl proton at 2.48 ppm in PEG-*b*-PC(P), and the appearance of the triazole proton resonance at 7.68 ppm and shifting of the vicinal methylenic protons in PEG-*b*-PC(Cou) (Figure S5). Besides, disappearance of the C_{sp}-H and C_{sp}-C_{sp} stretching bands at 3300 cm^{-1} and 2096 cm^{-1} of the side alkynyl groups was verified by FTIR in KBr matrix (Figure S6). FTIR (KBr, υ cm^{-1}): 3146, 3045 (Csp^2–H), 1739 (C=O), 1607 (C=C). ^{1}H NMR (400 MHz, $CDCl_3$, δ, ppm): 7.68 (s), 7.29 – 7.23 (m), 6.6–6.52 (m), 6.40 (s), 5.98 (s), 5.25–5.07 (m), 4.30 (t, *J* = 7.2 Hz), 4.15 (s), 3.76–3.45 (m), 3.47–3.31 (m), 2.37 (t, *J* = 7.2 Hz), 1.93–1.81 (m), 1.70–1.58 (m), 1.38–1.24 (m), 1.2 –1.05 (m).

2.3. Preparation of Self-Assemblies in Water

Milli-Q® water was gradually added to a solution of the copolymer (5 mg) in spectroscopic grade THF (1 mL) previously filtered through a 0.2 μm Teflon filter. The self-assembly process was monitored from the loss of transmitted light intensity at 650 nm due to scattering as a function of water content. When a constant value of turbidity

was reached, the resulting suspension was filtered through a 5 μm cellulose acetate filter and subjected to dialysis for 48 h against water to remove THF using a Spectra/Por dialysis membrane (MWCO, 1 kDa). Water suspensions of the polymeric self-assemblies with concentrations between 1.5–2.0 mg mL^{-1} were obtained.

2.4. Nile Red encapsulation and determination of the critical aggregation concentration

Critical aggregation concentration (CAC) was determined by fluorescence spectroscopy using Nile Red. Samples were prepared by introduction a stock solution of Nile Red in dichloromethane (87 μL, 3.7×10^{-5} M) to a vial and the solvent evaporated. Then, the micelles suspension with a concentration ranging from 1.0×10^{-4} to 1.0 mg/mL (600 μL) was added. The mixture was stirred overnight in orbital shaker. The emission spectra of Nile Red were registered from 560 to 700 nm while exciting at 550 nm.

2.5. Irradiation experiments

Irradiation experiments at 365 nm. Samples at a copolymer concentration of 1 mg mL^{-1} were placed in a quartz quvette and irradiated at 365 nm and 30 mW cm^{-2} with a Dymax 2000-EC lamp equipped with a glass UV filter. At different time intervals the sample was removed from the lamp, measuring Nile Red and coumarin unit emission in a fluorescence spectrophotometer.

Irradiation experiments at 730 nm. Samples were irradiated with 730 nm light using a Chameleon Ultra II Ti:Sapphire laser installed on a confocal microscope . Nominal power at 730 nm was around 2 W, the pulse width being 140 fs, at a frequency of 80Mhz. A PDMS stencil with circular wells (4 mm×350 μm, Alvéole) was stuck in a 23 mm glass bottom dish. Each well was filled with 5 μL of micellar solution (1 mg mL^{-1} polymer concentration). To avoid evaporation of the samples, the stencil was covered

with a 20 mm diameter coverslip and a small amount of water was deposited on the outer ring of the dish, then, the dish itself was sealed with parafilm. Irradiation with 730 nm light and measurement of Nile Red emission were performed by acquiring alternatively 3D stacks irradiating first at 730 nm (coumarin photoscission) and then at 514 nm (Nile Red excitation) every 10 min up to15 h.

2.6. Techniques

Fourier transform infrared spectroscopy (FTIR) was applied using a Bruker Tensor 27 FT-IR spectrophotometer and KBr disks. NMR experiments were carried out on Bruker Avance spectrometers operating at 400 or 300 MHz for ^{1}H, and 100 or 75 MHz for ^{13}C, using standard pulse sequences. Chemical shifts are given in ppm relative to TMS and the solvent residual peak was used as internal reference. Relative average molar masses (M_n^{SEC}) and dispersity ($Đ$) values were determined by size exclusion chromatography (SEC) using a Waters 2695 liquid chromatography system equipped with a Waters 2998 photodiode array and a Waters 2420 evaporation light scattering detectors using two Ultrastyragel columns with pore size of 500 and 10^4 Å calibrated using poly(methyl methacrylate) standards and THF as solvent.

UV−vis absorption spectra were recorded in a Varian Carey 4000 spectrophotometer. Fluorescence measurements were performed using a Hitachi F-7000 fluorescence spectrophotometer.

Dynamic light scattering (DLS) measurements were carried out in a Malvern Instrument Nano ZS using a He−Ne laser with a 633 nm wavelength and a detector angle of 173° at 25 °C. Samples were measured at 0.10 mg mL^{-1} concentration of the polymer. Hydrodynamic diameters (D_h) measurements were given as an average of three measures on each sample to ensure reproducibility.

The morphology of the micelles was investigated by transmission electron microscopy (TEM) using a JEOL JEM-2100 LaB_6 transmission electron microscope operating at a voltage of 200 kV. A small amount of the micellar dispersion (1 mg mL^{-1} polymer concentration) was placed onto a holey carbon TEM grid (Plano S147-4), dried at room temperature with a tissue and imaged. For Cryo-TEM inspection, 3 µL of the solution were placed on a holey carbon film (Plano S147-4), plotted for 2 s and plunged into liquid ethane using a Gatan CP3 cryo-plunger operating at T = 108 K. The frozen sample was transferred under liquid nitrogen to a cryo-TEM sample holder (Gatan 914) and investigated at T = 100 K and 200 kV accelerating voltage under low-dose settings using a JEOL JEM-2100 LaB_6 Transmission Electron Microscope.

Irradiation experiments at 730 nm were carried out inside a Zeiss LSM 880 confocal microscope equipped with a 10× Plan Neofluar objective with the image size set to 512×512 pixel (850×850 µm) and the dwell time set to 8.2 µs, with a pinhole size of 100µm. The light exposed volume of the sample corresponded to 6.8% of the total amount of solution.

3. Results and discussion

3.1. Synthesis of supramolecular and covalent coumarin functionalized amphiphilic block copolymers

2,2-Bis(hydroxymethyl)propionic acid (bis-MPA) is a versatile building block from which a cyclic carbonate monomer can be obtained by ring closure with ethyl chloroformate, also esterified with either propargyl or allyl alcohols, and polymerized by ROP with a high level of control [38,47,54]. A BC precursor consisting of a poly(ethylene glycol) hydrophilic segment and a polycarbonate with pendant double bonds, PEG-*b*-PC(A), was prepared by ROP of the allylic cyclic carbonate

5-methyl-5-allyloxycarbonyl-1,3-dioxan-2-one, MC(A), in dichloromethane using poly(ethylene glycol) methyl ether with an average molar mass of 5000 g mol^{-1} (PEG-OH) as the macroinitiator, and the organocatalytic system 1-(3,5-bis(trifluoromethyl)phenyl)-3-cyclohexylthiourea (TU)/1,8-diazabicyclo(5,4,0)undec-7-ene (DBU). It has been described that the metal-free catalytic system TU/DBU promotes fast polymerization rates and good control of the ROP for bis-MPA cyclic carbonates limiting concerns about metallic contaminants [54-56]. Full details are given in the Supporting Information.

The copolymer PEG-*b*-PC(DAP) with lateral DAP residues in the polycarbonate block was obtained by thiol-ene reaction. Both thermal (using AIBN as radical initiator) and light initiated (using DMPA as UV photoinitiator) thiol-ene reactions were tested with thiol:ene proportions ranging from 1:1 to 5:1. The progress of the functionalization of the polymeric backbone was followed by the disappearance of the allyl signals at 5.89 and 5.28 ppm in the ^{1}H NMR spectrum, and by the appearance of new signals at 2.88 and 2.58 ppm corresponding to the methylenic protons close to the thioether group (Figure S1). Quantitative conversion of the vinyl groups according to ^{1}H-NMR sensitivity was achieved only under UV light initiation with thiol:ene proportions equal or above to 2:1. Size exclusion chromatography (SEC) analysis for PEG-*b*-PC(A) and PEG-*b*-PC(DAP) revealed monomodals narrows distributions with a dispersity value of $Đ$ = 1.05 (Figure S2).

The corresponding coumarin functionalized supramolecular copolymers, were formed by DAP/T paring by dissolving PEG-*b*-PC(DAP) and T_nCou (n = 1, 5, 10) precursors in THF and subsequent slow evaporation of the solvent under continuous shaking at room temperature. Different spacers between the thymine unit and the

light-responsive coumarin unit were tested and the corresponding the supramolecular polymers were tagged as PEG-*b*-PC(DAP/T_nCou), (n = 1, 5, 10) (Figure 1). Molar ratios of both precursors were calculated to functionalize 95% of the DAP units with T_nCou, to avoid an excess of T_nCou. H-bond formation in the bulk solid material was assessed by FTIR by the modification of the C=O and N-H amide bands, of PEG-*b*-PC(DAP), T_nCou and PEG-*b*-PC(DAP/T_nCou) (Figure S3 for PEG-*b*-PC(DAP/T_1Cou). H-bond formation was also observed by ^{1}H NMR in $CDCl_3$ solution, as the protons involved in the hydrogen bonds shifted to lower fields (Figure S4 for PEG-*b*-PC(DAP/T_1Cou)).

The reference covalent functionalized copolymer, PEG-*b*-PC(Cou), was obtained by reaction of the alkynyl side groups of PEG-*b*-PC(P) with the azide N_3-Cou *via* CuAAC using the catalytic system CuBr/*N,N,N′,N″,N″*-pentamethyldiethylenetriamine (PMDETA) (Figure 1) [48,49]. In this case, the covalent incorporation of the coumarin by a photoinitiated thiol-ene postpolymerization reaction was discarded to prevent its premature photolysis under UV illumination. Extension of the postpolymerization modification was assessed by ^{1}H NMR and FTIR in KBr disk (see Figure S5 and S6) (Full details are given in Experimental Section). Postpolymerization functionalization was considered quantitative, taking into account the sensitivity of both spectroscopic techniques. SEC traces of PEG-*b*-PC(Cou) showed a distribution peak shifted to lower retention times compared to PEG-*b*-PC(P), due to the increase in the mass of the copolymer, with a dispersity value $Đ$ = 1.08 (Figure S7).

The quantitative scission of the photolabile coumarin ester bond was confirmed by ^{1}H NMR (DMSO-d^6) after 60 min by irradiation with UV light (365 nm, 30 mW cm^{-2}) for both PEG-*b*-PC(Cou) (Figure S15) and T_1Cou (Figure S16).

3.2. Self-assembly in water and characterization of the self-assemblies

Self-assembly of PEG-*b*-PC(DAP/T_nCou) and PEG-*b*-PC(Cou) was promoted by solvent switching starting from THF solutions of the polymers and gradually adding water. The preparation of stable micellar solutions from the supramolecular polymers PEG-*b*-PC(DAP/T_nCou) was strongly dependent on the length of the alkyl spacer connecting the coumarin to the thymine. Polymers with long spacers (n = 5, 10) formed a macroscopic precipitate during the self-assembly process, while polymer with a shorter spacer (n = 1) formed a stable micellar solution. Therefore, only supramolecular copolymer with n=1, PEG-*b*-PC(DAP/T_1Cou), and the covalent model, PEG-*b*-PC(Cou) were further investigated. Critical aggregation concentration (CAC) values determined by fluorescence spectroscopy experiments using Nile Red were 20 μg mL^{-1} for PEG-*b*-PC(DAP/T_1Cou) and 32 μg mL^{-1} for PEG-*b*-PC(Cou) (Figure S8). According to transmission electron microscopy (TEM) images, both PEG-*b*-PC(DAP/T_1Cou) and PEG-*b*-PC(Cou) formed spherical micelles with diameters around 25 nm (Figure 2). Micellar dispersions were analysed at room temperature by dynamic light scattering (DLS) showing monomodal size distribution curves with average hydrodynamic diameters (D_h) of 23 nm for PEG-*b*-PC(DAP/T_1Cou) and 28 nm for PEG-*b*-PC(Cou) (Figure 2). The samples were monitored up to 3 weeks showing almost constant D_h values along this period and not signs of precipitation (Figure S9 for PEG-*b*-PC(DAP/T_1Cou) and S10 for PEG-*b*-PC(Cou)). Overall results suggest a similar thermodynamic and temporal stability of the supramolecular and covalent block copolymers micellar self-assemblies, validating the H-bond anchoring of the coumarin by hydrogen bonding as a suitable strategy to access responsive nanocarriers from amphiphilic BCs. Even so, the lower values of CAC point to a slightly higher stability of the supramolecular micelles against dilution.

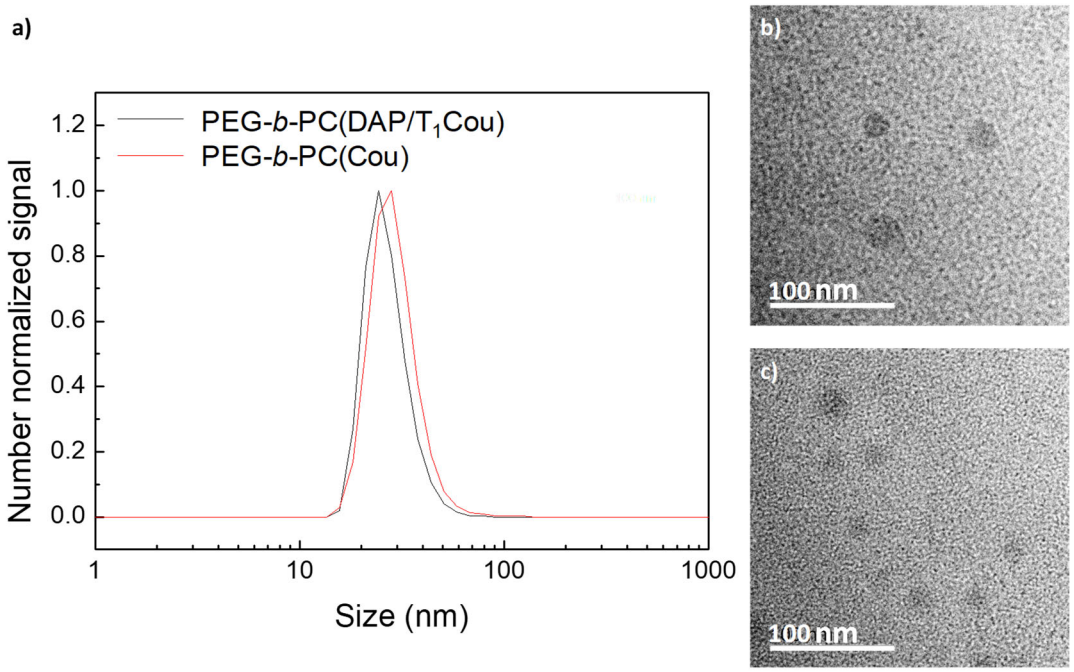

Figure 2. Number particle size distribution determined by DLS for PEG-*b*-PC(DAP/T$_1$Cou) and PEG-*b*-PC(Cou) (a), TEM images of PEG-*b*-PC(DAP/T$_1$Cou) (b), and PEG-*b*-PC(Cou) (c).

UV-Vis and fluorescence spectra of the aqueous micelle dispersions were measured and compared with those in THF solution (Figure 3). Similar spectra profiles were recorded for PEG-*b*-PC(DAP/T$_1$Cou) and PEG-*b*-PC(Cou), since the main spectral features are associated with the absorption/emission properties of the coumarin unit. A strong absorption band of the coumarin group was visible at 370 nm in THF. This band broaden and red shifted in the aqueous micelles dispersion, in particular in the supramolecular copolymer. A strong emission was observed at 450 nm in THF (λ_{exc}=370 nm) due to the coumarin. In the aqueous micellar dispersions, this emission was quenched due to the high local concentration of the coumarin inside of the micelle core [28]. A shift of the emission band was observed for the aqueous micellar suspensions, from 450 to 489 nm for PEG-*b*-PC(DAP/T$_1$Cou) and to 475 nm for PEG-*b*-PC(Cou).

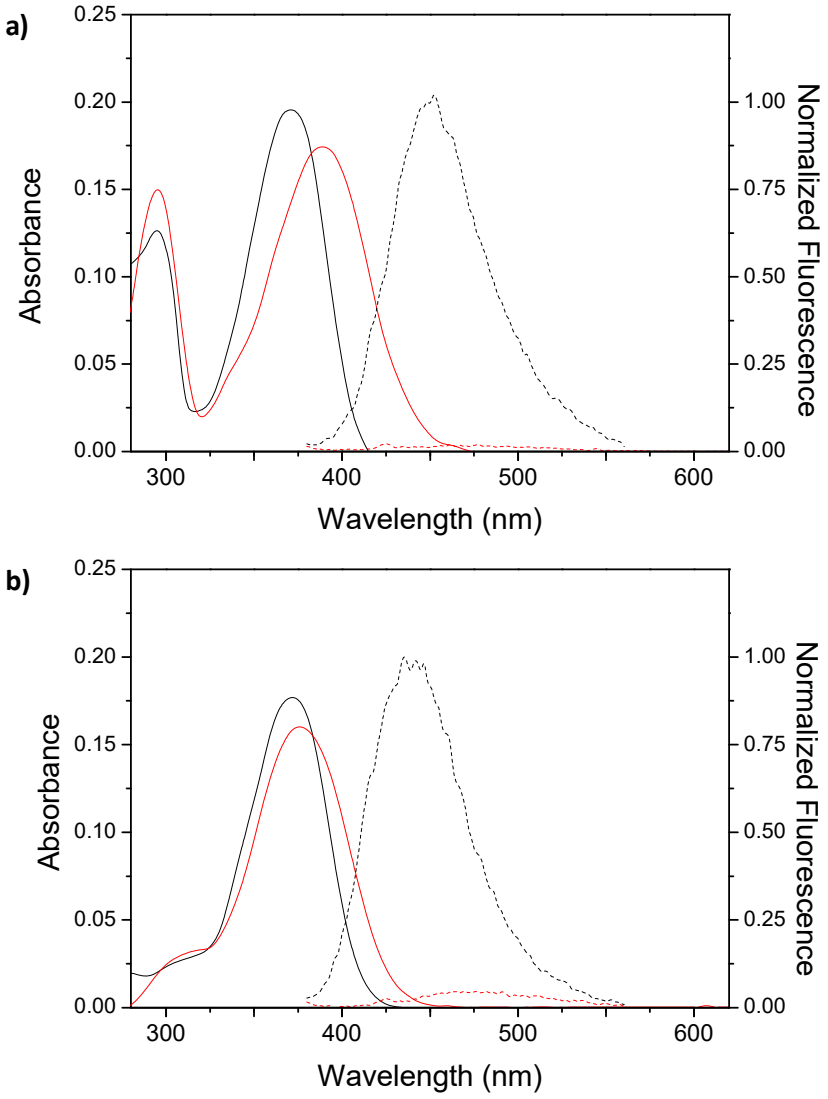

Figure 3. UV-Vis (solid line) and emission (dashed line) spectra in THF solution (black) and of the micellar dispersion in water (red) of (a) PEG-*b*-PC(DAP/T$_1$Cou) and (b) PEG-*b*-PC(Cou). Concentration of coumarin units was adjusted to about 10^{-4} M for UV-vis spectra and 10^{-6} M for emission spectra for both copolymers.

3.3. Release properties of photoresponsive micelles

Nile Red was selected as a fluorescent probe for our studies. This chromophore has an intense emission (λ_{exc}=550 nm) at 620 nm in nonpolar media, and the emission is quenched in polar environments. The emission spectra of Nile Red loaded micellar

dispersions (Figure S11 for PEG-*b*-PC(DAP/T_1Cou) and S12 for PEG-*b*-PC(Cou)) showed two weak emission peaks when exciting at 370 nm. The highest energy one at approx. 480 nm corresponded to the above described emission of the coumarin. The lowest energy one at 620 nm was the Nile Red emission band due to a nonradiative energy transfer process from the excited coumarin to encapsulated Nile Red as they are both closely packed at the core of the micelle [28]. Consistently, the emission band located at 620 nm was not observed upon excitation at 370 nm of plain micelles that were not loaded with Nile Red (Figure S11 for PEG-*b*-PC(DAP/T_1Cou) and S12 for PEG-*b*-PC(Cou)).

Nile Red loaded micelles showed almost identical sizes and morphologies than unloaded ones. Changes on size and morphology of the Nile Red loaded micelles upon light illumination were tracked by TEM and DLS. After exposure at 365 nm for 40 min the initial spherical micelles of the covalent copolymer PEG-*b*-PC(Cou) appeared as smashed and larger micellar structures (Figure 4). By DLS, the average D_h increased from 28 nm to 70 nm after UV light irradiation. Therefore, photolysis reaction of the coumarin at the micelles core that converts the ester group of the polycarbonate block into a carboxylic group does not lead to disassembly. Instead, the decrease of hydrophobicity of the polycarbonate block conducts to a significant swelling of the micelles, as of observed for acid labile polycarbonate micelles [57].

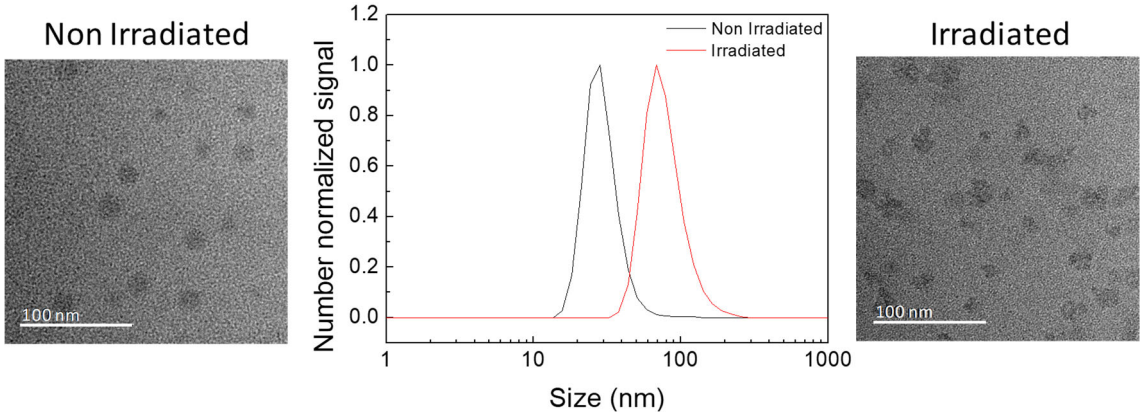

Figure 4. Number particle size distribution determined by DLS and TEM images before (left) and after (right) 40 min 365 nm irradiation of PEG-*b*-PC(Cou) self-assemblies.

The TEM images of irradiated micelles of PEG-*b*-PC(DAP/T$_1$Cou) showed a slight alteration of the surface while non-significant changes were detected in DLS measurements (Figure 5). Therefore, we conclude that the photodissociation of T$_1$Cou (to generate the thymine unit T$_1$COOH and release of Cou, see Figure S16) unit did not induce acute changes in the morphology of the self-assemblies of this block copolymer. To interpret these observations self-assemblies of the polymer PEG-*b*-PC(DAP/T$_1$COOH) were prepared. Spherical micelles of similar sizes and morphology to PEG-*b*-PC(DAP/T$_1$Cou) were obtained, suggesting that after the photocleavage of the thymine-coumarin unit, T$_1$Cou, the polymeric aggregates allowed reassembly of the polymer into micelles of similar sizes (Figure S13).

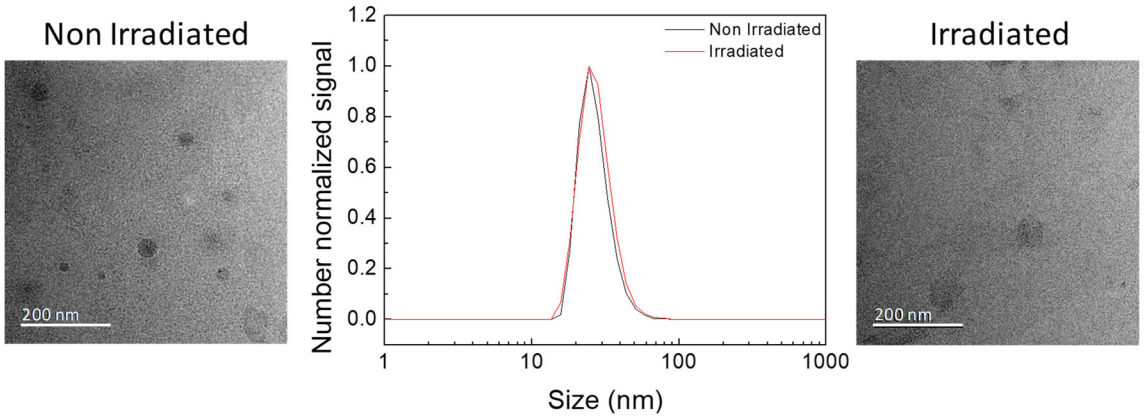

Figure 5. Number particle size distribution determined by DLS and TEM images before (left) and after (right) 40 min 365 nm irradiation of PEG-*b*-PC(DAP/T_1Cou) self-assemblies.

Nile Red loaded micelles were irradiated at 365 nm (30 mW cm^{-2}) for different time intervals and the changes on the emission of fluorophores were monitored upon excitation of the coumarin unit at 370 nm or Nile Red at 550 nm. When micelles dispersions were irradiated at 365 nm (30 mW cm^{-2}), the coumarin emission band at 480 nm increased steadily due to photoscission and diffusion of the coumarins from the micelles core, and minimization of coumarin self-quenching (Figure S14) [28]. After 40 min, an increase in the coumarin unit emission of a 60% for PEG-*b*-PC(DAP/T_1Cou) and 360% for PEG-*b*-PC(Cou) was measured, consistent with the more acute morphological changes registered for PEG-*b*-PC(Cou).

Figure 6 shows the evolution of the Nile Red emission upon 550 excitation of irradiated samples irradiated and the non irradiated ones taken as reference. In the case of the non irradiated micelles of covalent and supramolecular BCs, emission was almost constant in the studied range of time, evidencing that Nile Red is not released by a physical diffusion process. Under exposure at 365 nm, an abrupt decrease in emission was observed after 100 s for the covalent PEG-*b*-PC(Cou), as Nile Red environment

becomes more polar. In the case of PEG-*b*-PC(DAP/T_1Cou) the decrease in emission was more gradual, as expected from the less acute morphological changes in the supramolecular copolymer than in the covalent model. Because UV light irradiation did not induced a drastic disruption of the micellar morphology (Figure 4 and Figure 5), it should be expected that a mainly hydrophobic core was maintained after coumarin release. Under this premise, decrease of the Nile Red emission should be more likely related with the release, at least partial, of the probe to the surrounding polar medium than with a shift in the polarity of the hydrophobic block induced by the photoscission of the coumarin ester unit. These results are in accordance with the previously described by Zhao and coworkers, which described Nile Red release under similar conditions on covalent copolymers [28,29]. The final normalized Nile Red emission was similar for PEG-*b*-PC(DAP/T_1Cou) and PEG-*b*-PC(Cou), though longer exposure times were required in the case of the supramolecular copolymer to achieve it due to a slower emission decrease.

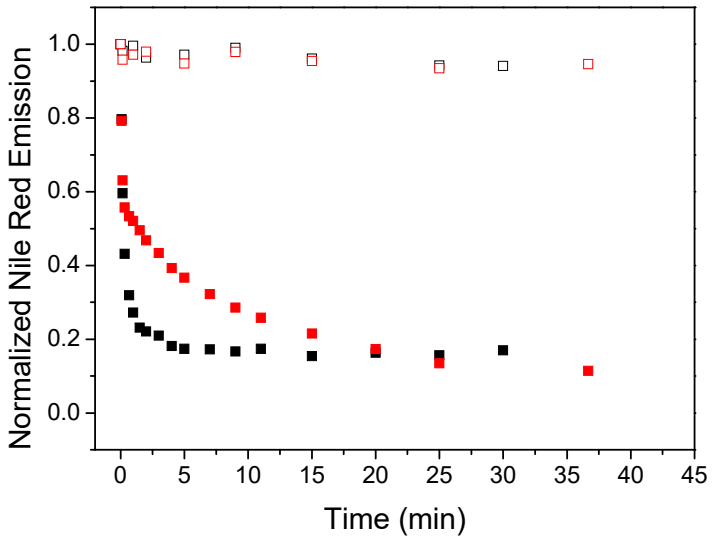

Figure 6. Normalized emission of Nile Red *vs* UV irradiation time for PEG-*b*-PC(DAP/T$_1$Cou) (solid red for the irradiated sample and hollow red for reference) and PEG-*b*-PC(Cou) (solid black for the irradiated sample and hollow black for reference).

Once the behavior of PEG-*b*-PC(Cou) and PEG-*b*-PC(DAP/T$_1$Cou) under UV-light stimulation was established, similar experiments were performed using NIR illumination. Samples were exposed to 730 nm light using a Chameleon Ultra II Ti:Sapphire laser (nominal power around 2 W at 730 nm) at laser power 10 or 20%. Emission of the Nile Red at 620 nm was monitored *in situ* (λ_{exc}=514 nm). Initially, a reference experiment was carried out to determine the stability of the Nile Red at 514 nm at the illumination conditions. A decrease of the emission intensity was detected, which we associated to photobleaching of Nile Red (see Figure 7, reference in blue). When micelles in aqueous media were exposed to 730 nm light, the emission intensity decreased steadily when increasing the irradiation time. This decay was twice as fast when doubling the laser power (see Figure 7). The NIR-induced response of the Nile Red micelles was slower than with UV irradiation. This is attributed to the lower efficiency inherent to

two-photon processes. Again, different Nile Red emission profiles were observed for the covalent and supramolecular block copolymer, being slower for PEG-*b*-PC(DAP/T$_1$Cou) in agreement with Nile Red emission evolution observed under 365 nm stimulation.

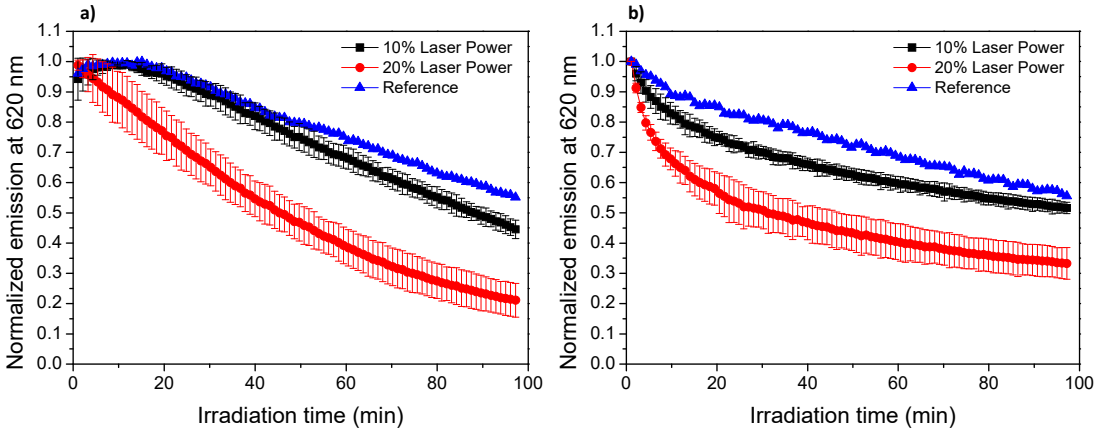

Figure 7: Normalized emission of Nile Red emission evolution versus NIR irradiation time (min) for: (a) PEG-*b*-PC(DAP/T$_1$Cou) and (b) PEG-*b*-PC(Cou).

4. Conclusions

Two amphiphilic diblock copolymers formed by hydrophilic PEG and hydrophobic aliphatic polycarbonate have been prepared by organocatalyzed ROP. The light responsive unit [7-(diethylaminocoumarin)-4-yl]methyl ester was introduced in the side chain of the polycarbonate block either by a supramolecular or a covalent approach, taking the covalent copolymer as a model reference. Both supramolecular and covalent copolymers were able to self-assemble into spherical micelles of about 25 nm diameter when dispersed in water. After irradiation at 365 nm, the photoscission of the coumarin unit induced morphological changes in the micelles.

The capability of these materials to encapsulate small molecules was demostrated by encapsulating a hydrophobic fluorescent molecular probe, Nile Red. Both UV and

NIR stimulation induced the release of Nile Red to the surrounding media. The release was more gradual for the supramolecular block copolymer. NIR induced release took longer exposure doses due to the lower efficiency of two photon processes, though the relative final Nile Red emission values were similar for UV- and NIR-stimulated release for both covalent and supramolecular copolymers. Therefore, introduction of the light-responsive unit by hydrogen bonding proved to be a suitable strategy to obtain light-responsive nanocarriers with photoresponse properties comparable to the reference covalent materials but with a lower synthetic effort.

In summary, the work demonstrates that this H-bonding based supramolecular postpolymerization functionalization is optimal not only for the design of light stimulable nanocarriers based on the photoisomerization of azobenzenes but also for those based on photocleavable bonds with more significant light induced chemical changes. Thus, a synthetic approach providing high flexibility in the functional polymeric materials design is combined with the response to NIR light of interest in biomedical applications for which UV light is not recommended.

Funding

This work was funded by the Ministerio de Economia y Competitividad (MINECO)-FEDER, under the project grant number MAT2017-84838-P, and Gobierno de Aragon-FEDER (Liquid Crystals and Polymers Group E47_17R, FEDER 2014-2020 "Construyendo Europa desde Aragón").

Acknowledgements

Alejandro Roche acknowledges MINECO (BES-2015-071235) for his PhD grant. Authors would like to thank Dr. Marcus Koch from Leibniz Institut für neue Materialien

- INM for his kind help with TEM measurments. Alejandro Roche would like to thank Stefan Brück and Dr. Julieta I. Paez for his invaluable help during his stay at INM. The authors acknowledge the Centro de Química y Materiales de Aragón, CEQMA (CSIC,Universidad de Zaragoza) for the NMR facilities. The authors additionally would like to acknowledge the use of the Servicio General de Apoyo a la Investigacion, SAI, of the Universidad de Zaragoza.

Appendix A. Supplementary material

Supplementary data to this article can be found online

Data availability

The raw/processed data required to reproduce thesefindings cannotbe shared at this time as the data also forms part of an ongoing study.

References

[1] J. Panyam, V. Labhasetwar, Biodegradable nanoparticles for drug and gene delivery to cells and tissue, Adv. Drug Deliv. Rev. 55 (2013) 329–347. https//doi.org/10.1016/S0169-409X(02)00228-4.

[2] . Chen, I. Roy, C. Yang, P.N. Prasad, Nanochemistry and nanomedicine for nanoparticle-based diagnostics and therapy, Chem. Rev. 116 (2016) 2826–2885. https//doi.org/10.1021/acs.chemrev.5b00148.

[3] H. Cabral, K. Miyata, K. Osada, K. Kataoka, Block copolymer micelles in nanomedicine applications, Chem. Rev. 118 (2018) 6844–6892. https//doi.org/10.1021/acs.chemrev.8b00199.

[4] J. del Barrio, L. Oriol, M. Piñol, Light-controlled encapsulation and release enabled by photoresponsive polymer self-assemblies, in: Q. Li (Ed), Photoactive Functional Soft Materials: Preparation, Properties, and Applications, Wiley-VCH, Weinheim, 2019, pp. 413–448. https//doi.org/10.1002/9783527816774.

[5] J. Yin, Y. Chen, Z.-H. Zhang, X. Han, Stimuli-responsive block copolymer-based assemblies for cargo delivery and theranostic applications, Polymers 8 (2016) 268. https//doi.org/10.3390/polym8070268.

[6] Y. Chang, Y. Jiao, H.E. Symons, J.-F. Xu, C.F.J. Faul, X. Zhang, Molecular engineering of polymeric supra-amphiphiles. Chem. Soc. Rev. 48 (2019) 989–1003. https//doi.org/10.1039/C8CS00806J.

[7] M. Elsabahy, K.L. Wooley, Design of polymeric nanoparticles for biomedical delivery applications, Chem Soc Rev 41 (2012) 2545–2561. https//doi.org/10.1039/c2cs15327k.

[8] M. Yokoyama, Polymeric micelles as a new drug carrier system and their required considerations for clinical trials, Expert. Opin. Drug Deliv. 7 (2010) 145–158. https//doi.org/10.1517/17425240903436479.

[9] S.C. Owen, D.P.Y. Chan, M.S. Shoichet, Polymeric micelle stability, Nano Today 7 (2012) 53–65. https//doi.org/10.1016/j.nantod.2012.01.002.

[10] .A. Figg, R.N. Carmean, K.C. Bentz, S. Mukherjee, D.A. Savin, B.S. Sumerlin, Tuning hydrophobicity to program block copolymer assemblies from the inside out, Macromolecules 50 (2017) 935–943. https//doi.org/10.1021/acs.macromol.6b02754.

[11] U. Tritschler, S. Pearce, J. Gwyther, G.R. Whittell, I. Manners, 50th Anniversary perspective : functional nanoparticles from the solution self-assembly of block copolymers, Macromolecules 50 (2017) 3439–3463. https//doi.org/10.1021/acs.macromol.6b02767.

[12] Y. Huang, R. Dong, X. Zhu, D. Yan, Photo-responsive polymeric micelles, Soft Matter. 10 (2014) 6121–6138. https//doi.org/10.1039/C4SM00871E.

[13] Y. Zhou, H. Ye, Y. Chen, R. Zhu, L. Yin, Photoresponsive drug/gene delivery systems, Biomacromolecules 19 (2018) 1840–1857. https//doi.org/10.1021/acs.biomac.8b00422.

[14] P. Xiao, J. Zhang, J. Zhao, M.H. Stenzel, Light-induced release of molecules from polymers, Prog. Polym. Sci. 74 (2017) 1–33. https//doi.org/10.1016/j.progpolymsci.2017.06.002.

[15] N. Fomina, J. Sankaranarayanan, A. Almutairi, Photochemical mechanisms of light-triggered release from nanocarriers, Adv Drug Deliv. Rev. 64 (2012) 1005–1020. https//doi.org/10.1016/j.addr.2012.02.006..

[16] Y. Zhao, Light-responsive block copolymer micelles, Macromolecules 45 (2012) 3647–3657. https//doi.org/10.1021/ma300094t.

[17] A. Concellón, E. Blasco, A. Martínez-Felipe, J.C. Martínez, I. Šics, T.A. Ezquerra, A. Nogales, M. Piñol, L. Oriol, Light-responsive self-assembled materials by supramolecular post-functionalization via hydrogen bonding of amphiphilic block copolymers, Macromolecules 49 (2016) 7825–7836. https//doi.org/10.1021/acs.macromol.6b01112.

[18] Y. Xia, Y. Zeng, D. Hu, H. Shen, J. Deng, Y. Lu, X. Xia, W. Xu, Light and pH dual-sensitive biodegradable polymeric nanoparticles for controlled release of cargos, J. Polym. Sci. Part A: Polym. Chem. 55 (2017) 1773–1783. https//doi.org/10.1002/pola.28528.

[19] Hu D, Peng H, Niu Y, Li Y, Xia Y, Li L, He J, Liu X, Xia X, Lu Y, Xu W. Reversibly light-responsive biodegradable poly(carbonate) micelles constructed via CuAAC reaction. J Polym Sci Part A Polym Chem 2015;53:750–760. https//doi.org/10.1002/pola.27499.

[20] H.-J. Kim, H. Lee, Polymeric micelles based on light-responsive block copolymers for the phototunable detection of mercury(II) ions modulated by morphological

changes, ACS Appl. Mater. Interfaces 10 (2018) 34634–34639. https//doi.org/10.1021/acsami.8b12441.

[21] F. Sun, P. Zhang, Y. Liu, C. Lu, Y. Qiu, H. Mu, J. Duan, A photo-controlled hyaluronan-based drug delivery nanosystem for cancer therapy, Carbohydr. Polym. 206 (2019) 309–318. https//doi.org/10.1016/j.carbpol.2018.11.005.

[22] L. Beauté, N. McClenaghan, S. Lecommandoux, Photo-triggered polymer nanomedicines: From molecular mechanisms to therapeutic applications, Adv. Drug Deliv. Rev. 138 (2019) 148–166. https//doi.org/10.1016/j.addr.2018.12.010.

[23] X. Zeng, X. Zhou, S. Wu, Red and near-infrared light-cleavable polymers, Macromol. Rapid. Commun. 30 (2018) 1800034. https//doi.org/10.1002/marc.201800034.

[24] H.J. Cho, M. Chung, M.S. Shim, Engineered photo-responsive materials for near-infrared-triggered drug delivery, J. Ind. Eng. Chem. 31 (2015) 15–25. https//doi.org/10.1016/j.jiec.2015.07.016.

[25] J.L. Mynar, A.P. Goodwin, J.A. Cohen, Y. Ma, G.R. Fleming, J.M.J. Fréchet, Two-photon degradable supramolecular assemblies of linear-dendritic copolymers, Chem. Commun. (2017) 2081–2082. https//doi.org/10.1039/B701681F.

[26] L. Sun, Y. Yang, C.-M. Dong, Y. Wei, Two-photon-sensitive and sugar-targeted nanocarriers from degradable and dendritic amphiphiles, Small 7 (2011) 401–406. https//doi.org/10.1002/smll.201001729.

[27] J. Jiang, X. Tong, D. Morris, Y. Zhao, Toward photocontrolled release using light-dissociable block copolymer micelles, Macromolecules 39 (2006) 4633–4640. https//doi.org/10.1021/ma060142z.

[28] J. Babin, M. Pelletier, M. Lepage, J.-F. Allard, D. Morris, Y. Zhao, A New two-photon-sensitive block copolymer nanocarrier, Angew. Chem. Int. Ed. 48 (2009) 3329–3332. https//doi.org/10.1002/anie.200900255.

[29] S. Kumar, J.-F. Allard, D. Morris, Y.L. Dory, M. Lepage, Y. Zhao, Near-infrared light sensitive polypeptide block copolymer micelles for drug delivery, J. Mater. Chem. 22 (2012) 7252–7257. https//doi.org/10.1039/c2jm16380b.

[30] J.P. Roth, Composing Well-defined stimulus-responsive materials through postpolymerization modification reactions, Macromol. Chem. Phys. 215 (2014) 825–838. https//doi.org/10.1002/macp.201400073.

[31] M.A. Gauthier, M.I. Gibson, H.-A. Klok, Synthesis of functional polymers by post-polymerization modification, Angew. Chem. Int. Ed. 48 (2009) 48–58. https//doi.org/10.1002/anie.200801951.

[32] E. Blasco, M.B. Sims, A.S. Goldmann, B.S. Sumerlin, C. Barner-Kowollik, 50th Anniversary perspective : polymer functionalization, Macromolecules 50 (2017) 5215–5252. https//doi.org/10.1021/acs.macromol.7b00465.

[33] J. Romulus, J.T. Henssler, M. Weck, Postpolymerization modification of block copolymers, Macromolecules 47 (2014) 5437–5449. https//doi.org/10.1021/ma5009918.

[34] J.M. Pollino, M. Weck, Non-covalent side-chain polymers: design principles, functionalization strategies, and perspectives, Chem. Soc. Rev. 34 (2005) 193–207. https//doi.org/10.1039/b311285n.

[35] M. Weck, Side-chain functionalized supramolecular polymers, Polym. Int. 56 (2017) 453–460. https//doi.org/10.1002/pi.2200.

[36] R. McHale, R.K. O'Reilly, Nucleobase containing synthetic polymers: advancing biomimicry via controlled synthesis and self-assembly, Macromolecules 45 (2012) 7665–7675. https//doi.org/10.1021/ma300895u.

[37] F. Ilhan, M. Gray, V.M. Rotello, Reversible side chain modification through noncovalent interactions. 'Plug and play' polymers, Macromolecules 34 (2001) 2597–2601. https//doi.org/10.1021/ma001700r.

[38] G. Becker, F.R. Wurm, Functional biodegradable polymers *via* ring-opening polymerization of monomers without protective groups, Chem. Soc. Rev. 47 (2018) 7739–7782. https//doi.org/10.1039/C8CS00531A.

[39] Y. Dai, X. Zhang, Recent development of functional aliphatic polycarbonates for the construction of amphiphilic polymers, Polym. Chem. 8 (2017) 7429–7437. https//doi.org/10.1039/C7PY01815K.

[40] K. Fukushima, Poly(trimethylene carbonate)-based polymers engineered for biodegradable functional biomaterials, Biomater. Sci. 4 (2016) 9–24. https//doi.org/10.1039/C5BM00123D.

[41] J. Xu, E. Feng, J. Song, Renaissance of aliphatic polycarbonates: new techniques and biomedical applications: a review, J. Appl. Polym. Sci. 131 (2014) 39822. https//doi.org/10.1002/app.39822.

[42] S. Tempelaar, L. Mespouille, O. Coulembier, P. Dubois, A.P. Dove, Synthesis and post-polymerisation modifications of aliphatic poly(carbonate)s prepared by ring-opening polymerisation, Chem. Soc. Rev. 42 (2013) 1312–1336. https//doi.org/10.1039/C2CS35268K.

[43] A.W. Thomas, A.P. Dove, Postpolymerization modifications of alkene-functional polycarbonates for the development of advanced materials biomaterials, Macromol. Biosci. 16 (2016) 1762–1775. https//doi.org/0.1002/mabi.201600310.

[44] A.B. Lowe. Thiol–ene 'click' reactions and recent applications in polymer and materials synthesis: a first update, Polym. Chem. 5 (2014) 4820–4870. https//doi.org/10.1039/C4PY00339J.

[45] H. Kuang, S. Wu, Z. Xie, F. Meng, X. Jing, Y. Huang, Biodegradable amphiphilic copolymer containing nucleobase: synthesis, self-assembly in aqueous solutions, and potential use in controlled drug delivery, Biomacromolecules 13 (2012) 3004–3012. https//doi.org/10.1021/bm301169x.

[46] G. Delaittre, N.K. Guimard, C. Barner-Kowollik, Cycloadditions in modern polymer chemistry, Acc. Chem. Res. 48 (2015) 1296–1307. https//doi.org/10.1021/acs.accounts.5b00075.

[47] S. Tempelaar, I.A. Barker, V.X. Truong, D.J. Hall, L. Mespouille, P. Dubois, A.P. Dove, Organocatalytic synthesis and post-polymerization functionalization of propargyl-functional poly(carbonate)s, Polym. Chem. 4 (2013) 174–183. https//doi.org/10.1039/C2PY20718D.

[48] J. Royes, J. Rebolé, L. Custardoy, N. Gimeno, L. Oriol, R.M. Tejedor, M. Piñol, Preparation of side-chain liquid crystalline azopolymers by CuAAC postfunctionalization using bifunctional azides: induction of chirality using

circularly polarized light, J. Polym. Sci. Part A: Polym. Chem. 50 (2012) 1579–1590. https//doi.org/10.1002/pola.25929.

[49] A. Roche, H. García-Juan, J. Royes, L. Oriol, M. Piñol, B. Audia, P. Pagliusi, C. Provenzano, G. Cipparrone, Tuning the thermal properties of azopolymers synthesized by post-functionalization of poly(propargyl methacrylate) with azobenzene azides: influence on the generation of linear and circular birefringences. Macromol. Chem. Phys. 219 (2018) 1800318. https//doi.org/10.1002/macp.201800318.

[50] X. Hu, X. Chen, Z. Xie, S. Liu, X. Jing, Synthesis and characterization of amphiphilic block copolymers with allyl side-groups, J. Polym. Sci. Part A: Polym. Chem. 45 (2007) 5518–5528. https//doi.org/10.1002/pola.22297.

[51] C. Lu, Q. Shi, X. Chen, T. Lu, Z. Xie, X. Hu, J. Ma, X. Jing, Sugars-grafted aliphatic biodegradable poly(L-lactide-co-carbonate)s by click reaction and their specific interaction with lectin molecules, J. Polym. Sci. Part A: Polym. Chem. 45 (2007) 3204–3217. https//doi.org/10.1002/pola.22070.

[52] Q. Shi, X. Chen, T. Lu, X. Jing, The immobilization of proteins on biodegradable polymer fibers via click chemistry, Biomaterials 29 (2008) 1118–1126. https//doi.org/10.1016/j.biomaterials.2007.11.008.

[53] R.C. Pratt, B.G.G. Lohmeijer, D.A. Long, P.N.P. Lundberg, A.P. Dove, H. Li, C.G. Wade, R.M. Waymouth, J.L. Hedrick, Exploration, optimization, and application of supramolecular thiourea−amine catalysts for the synthesis of lactide (co)polymers, Macromolecules 39 (2006) 7863–7871. https//doi.org/10.1021/ma061607o.

[54] S. Tempelaar, L. Mespouille, P. Dubois, A.P. Dove, Organocatalytic synthesis and postpolymerization functionalization of allyl-functional poly(carbonate)s, Macromolecules 44 (2011) 2084–2091. https//doi.org/10.1021/ma102882v.

[55] Y. Qiao, C. Yang, D.J. Coady, Z.Y. Ong, J.L. Hedrick, Y.-Y. Yang, Highly dynamic biodegradable micelles capable of lysing Gram-positive and Gram-negative bacterial membrane, Biomaterials 33 (2012) 1146–1153. https//doi.org/10.1016/j.biomaterials.2011.10.020.

[56] R.C. Pratt, F. Nederberg, R.M. Waymouth, J.L. Hedrick, Tagging alcohols with cyclic carbonate: a versatile equivalent of (meth)acrylate for ring-opening polymerization, Chem. Commun. (2008) 114–116. https//doi.org/10.1039/B713925J.

[57] W. Chen, F. Meng, F. Li, S.J. Ji, Z. Zhong, pH-Responsive micelles based on acid-labile polycarbonate hydrophobe: synthesis and triggered drug release, Biomacromolecules 10 (2009) 1727-1735. https//doi.org/10.1021/bm900074d

Figure captions

Figure 1. Synthesis pathway of coumarin functionalized block copolymers.

Figure 2. DLS traces of PEG-*b*-PC(DAP/T_1Cou) and PEG-*b*-PC(Cou) (a), TEM images of PEG-*b*-PC(DAP/T_1Cou) (b), and PEG-*b*-PC(Cou) (c).

Figure 3. UV-Vis (solid line) and emission (dashed line) spectra in THF solution (black) and of the micellar dispersion in water (red) of (a) PEG-*b*-PC(DAP/T_1Cou) and (b) PEG-*b*-PC(Cou). Concentration of coumarin units was adjusted to about 10^{-4} M for UV-vis spectra and 10^{-6} M for emission spectra for both copolymers.

Figure 4. DLS traces and TEM images before (left) and after (right) 40 min 365 nm irradiation of PEG-*b*-PC(Cou) self-assemblies.

Figure 5. DLS traces and TEM images before (left) and after (right) 40 min 365 nm irradiation of PEG-*b*-PC(DAP/T_1Cou) self-assemblies.

Figure 6. Normalized emission of Nile Red *vs* UV irradiation time for PEG-*b*-PC(DAP/T_1Cou) (solid red for the irradiated sample and hollow red for reference) and PEG-*b*-PC(Cou) (solid black for the irradiated sample and hollow black for reference).

Figure 7: Normalized emission of Nile Red emission evolution versus NIR irradiation time (min) for: (a) PEG-*b*-PC(DAP/T_1Cou) and (b) PEG-*b*-PC(Cou).